Progress In Electromagnetics Research B, Vol. 38, 39–56, 2012

IMPROVED SHIFT-OPERATOR FDTD METHOD FOR ANISOTROPIC MAGNETIZED COLD PLASMAS WITH ARBITRARY MAGNETIC FIELD DECLINATION

X. Yin*, H. Zhang, H.-Y. Xu, and X.-F. Zeng

Radar Engineering Department, Missile Institute of Air Force Engineering University, Sanyuan, Shaanxi 713800, China

Abstract—In this paper, a recently improved SO-FDTD (shift-operator finite difference time-domain) method is proposed and applied to the numerical analysis of the anisotropic magnetized plasma with arbitrary magnetic declination. By using the constitutive relation between polarized current density vector **J** and electric vector **E** and bringing the shift operators, the difference iteration equations of field components for Maxwell equations are derived in detail. Furthermore, the memory requirement is decreased significantly through incorporating a memory-minimized algorithm into the FDTD iterative cycles. The reflection and transmission coefficients of electromagnetic wave through a magnetized plasma layer are calculated by using this method. It is shown that the new method not only improves accuracy but also produces speed and memory advantages over the SO-FDTD method in kDB coordinates system proposed in the recent reference. In addition, the recursion formulae of the improved SO-FDTD method are deduced and programmed easily and they involve no complex variables, so the computations for the magnetized plasma become very simple.

1. INTRODUCTION

The finite-difference time-domain (FDTD) method is a powerful tool for dealing with electromagnetic (EM) problems related to dispersive media and anisotropic media, such as magnetized plasma. During the past two decades, there have been numerous investigations of FDTD dispersive media formulations [1–15]. These include the recursive convolution FDTD (RC-FDTD) method [2], the piecewise-linear recursive convolution FDTD (PLRC-FDTD) method [3, 4],

Received 5 December 2011, Accepted 31 December 2011, Scheduled 9 January 2012

* Corresponding author: Xiong Yin (yinxiong325@hotmail.com).

the Z transform FDTD (ZT-FDTD) method [5, 6], the piecewise-linear current density recursive convolution FDTD (PLCDRC-FDTD) method [7], the trapezoidal recursive convolution finite-difference time-domain (TRC-FDTD) method [8, 9], the FDTD method based on locally one-dimensional scheme [6, 10, 11], the current-density-Laplace-transfer FDTD (CLT-FDTD) method [12] and the shift-operator finite-difference time-domain (SO-FDTD) method [13–15], and so on. The above FDTD methods have been mainly used to analyze EM problems for magnetized plasma where the external magnetic field direction is parallel to the direction of EM-wave propagation, which is a serious limitation. For many practical cases of interest, however, the angle between the external magnetic field direction and the direction of propagation is arbitrary [16–18]. In [16], the stopping power for arbitrary angle between the test particle velocity and magnetic field is investigated by using the longitudinal dielectric function derived for charged test particles in helical movement around magnetic field lines. H. B. Nersisyan et al. focus on the influence of a strong magnetic field with arbitrary angle of declination on the interactions between charged particles in a many-body system [17]. An ion projectile stopping at a velocity smaller than the target electron thermal velocity in a strong magnetic field is studied thoroughly in [18]. However, these research in [16–18] centralize on the charged particles in magnetic field and there are no numerical EM-models and related numerical methods, so we want to find an effective numerical method to solve the EM-problems in anisotropic medium with arbitrary magnetic field declination.

Several approaches have emerged that incorporate the FDTD algorithm into the numerical analysis of magnetized plasma with arbitrary magnetic declination. In [19] and [20], JE convolution FDTD (JEC-FDTD) method and PLRC-FDTD method are developed respectively to study the scattering and the transmission characteristics from the anisotropic magnetized plasma with arbitrary magnetic declination. These methods involve complicated convolutions and many exponential variables in the FDTD iteration equations. To avoid convolution calculation, the FDTD method based on Laplace transfer principle (CLT-FDTD) [21] is proposed to investigate the magnetized plasma with arbitrary magnetic declination. However, there are complicated conversions from the time-domain to the s-domain or from the s-domain to the time-domain in the CLT-FDTD method. Compared with the FDTD methods mentioned above, the SO-FDTD method has many advantages. First, there is no convolution calculation or complicated transforms, moreover, the conceptions of the SO-FDTD method are concise and the formulation derivations are simple. During the formulae derivation of the SO-FDTD method, the dielectric constants

or electric susceptibility of dispersive media in frequency-domain are written as a rational polynomial function and the constitutive relations between **D** and **E** or **J** and **E** are deduced in the time-domain. Through a shift operator, the constitutive relations in time-domain are transformed to the discrete time-domain. In [22], the SO-FDTD method is first introduced into the kDB coordinates system and the EM-problem model which covers all the respects of EM-problem for anisotropic plasma is set up, then the reflection and transmission coefficients of magnetized plasma slab are calculated. However, the required storage variables for each cell in the problem space are numerous due to the high order (the order is 4 or 6 in general) of the $j\omega$ in the rational polynomial function, so the FDTD iteration will take much memory and the computational efficiency is not high.

Different from the FDTD methods mentioned above, an improved SO-FDTD method for magnetized plasma with arbitrary magnetic declination is proposed and discussed in this paper. During the derivation of the formulations, we see some advantages of this method, such as easy derivation of formulae, clear concept and simplicity. Compared to the SO-FDTD method in kDB coordinates system proposed in [22], the proposed method not only improves the accuracy but also spends less machine time due to the great reduction of storage arrays for the problem space. The high efficiency and accuracy of this method are confirmed by computing the reflection and transmission coefficients of electromagnetic wave through a magnetized plasma layer with the biasing magnetic field at an arbitrary angle θ with respect to the direction of propagation.

2. METHODOLOGY

2.1. Electric Susceptibility Tensor of Magnetized Plasma

Considering the anisotropic magnetized cold plasma with collision and assuming that the external static magnetic field in Cartesian coordinate is in the y-z plane and declines an angle θ from z axis, the permittivity of the plasma must be a tensor [2, 15, 20] and it can be expressed as

$$\hat{\varepsilon}(\omega) = \varepsilon_0(\mathbf{I} + \hat{\chi}(\omega)) \tag{1}$$

where ε_0 is the permittivity in vacuum, $\mathbf{I}$ is a unit tensor and $\hat{\chi}$ is the electric susceptibility tensor. $\hat{\chi}$ can be written as [20]

$$\hat{\chi}(\omega) = [T] \begin{bmatrix} \chi_{11}(\omega) & \chi_{12}(\omega) & 0 \\ \chi_{21}(\omega) & \chi_{22}(\omega) & 0 \\ 0 & 0 & \chi_{33}(\omega) \end{bmatrix} [T]^{-1} \tag{2}$$

where

$$[T] = \begin{bmatrix} 0 & 1 & 0 \\ -\cos\theta & 0 & \sin\theta \\ \sin\theta & 0 & \cos\theta \end{bmatrix} \tag{3}$$

and the components of the electric susceptibility tensor are as follows:

$$\chi_{11}(\omega) = \chi_{22}(\omega) = \frac{-j\omega_p^2(j\omega + \nu_{en})}{\omega[(j\omega + \nu_{en})^2 + \omega_b^2]} \tag{4a}$$

$$\chi_{12}(\omega) = -\chi_{21}(\omega) = \frac{j\omega_p^2\omega_b}{\omega[(j\omega + \nu_{en})^2 + \omega_b^2]} \tag{4b}$$

$$\chi_{33}(\omega) = \frac{-j\omega_p^2}{\omega(j\omega + \nu_{en})} \tag{4c}$$

In these expressions, ω is the EM-wave angular frequency, $\omega_p (= 2\pi f_p)$ is the plasma angular frequency, ω_b is the cyclotron frequency (proportional to the static magnetic field $\mathbf{B}_0$) and ν_{en} is the collision frequency.

Substituting (3) into (2) and denoting any function $\chi_{ij}(\omega) = \chi_{ij}$, we get

$$\hat{\chi}(\omega) = \begin{bmatrix} \chi_{11} & \chi_{12}\cos\theta & -\chi_{12}\sin\theta \\ -\chi_{12}\cos\theta & \chi_{11}\cos^2\theta + \chi_{33}\sin^2\theta & (\chi_{33} - \chi_{11})\cos\theta\sin\theta \\ \chi_{12}\sin\theta & (\chi_{33} - \chi_{11})\cos\theta\sin\theta & \chi_{11}\sin^2\theta + \chi_{33}\cos^2\theta \end{bmatrix} \tag{5}$$

2.2. Derivation of the Improved SO-FDTD Formulations

In anisotropic magnetized plasma, Maxwell's curl equations are [7, 12, 15]:

$$\nabla \times \mathbf{E} = -\mu_0 \frac{\partial \mathbf{H}}{\partial t} \tag{6a}$$

$$\nabla \times \mathbf{H} = \varepsilon_0 \frac{\partial \mathbf{E}}{\partial t} + \mathbf{J} \tag{6b}$$

where $\mathbf{E}$, $\mathbf{H}$ and $\mathbf{J}$ are electric field vector, magnetic intensity vector and polarized current density vector respectively; μ_0 is magnetic permeability.

The grid configuration for $\mathbf{J}$ is to place J_x, J_y and J_z at the locations of E_x, E_y and E_z, respectively. If we define $\mathbf{E}$ at integer time steps, i.e., $\mathbf{E}^n$, while $\mathbf{H}$ and $\mathbf{J}$ at half integer time steps, i.e., $\mathbf{H}^{n+1/2}$ and $\mathbf{J}^{n+1/2}$, Equations (6) can be readily integrated into the FDTD

algorithm. Taking a component for example, the discrete difference schemes of (6) are

$$H_x^{n+\frac{1}{2}} = H_x^{n-\frac{1}{2}} - \frac{\Delta t}{\mu_0}(\nabla \times \mathbf{E})_x^n \tag{7}$$

$$E_x^{n+1} = E_x^n + \frac{\Delta t}{\varepsilon_0}(\nabla \times \mathbf{H})_x^{n+\frac{1}{2}} - \frac{\Delta t}{\varepsilon_0} J_x^{n+\frac{1}{2}} \tag{8}$$

where Δt is the time step. By the same procedure, other components can be easily obtained too.

The constitutive relation between polarized current density vector and electric field vector is [15]

$$\mathbf{J} = j\omega\varepsilon_0\hat{\chi} \cdot \mathbf{E} \tag{9}$$

When Equation (9) is expanded, combined with Equation (5), the component expressions of $\mathbf{J}$ are as follows:

$$\begin{aligned} J_x(\omega) = {} & j\omega\chi_{11} \cdot \varepsilon_0 E_x(\omega) + j\omega\chi_{12}\cos\theta \cdot \varepsilon_0 E_y(\omega) \\ & - j\omega\chi_{12}\sin\theta \cdot \varepsilon_0 E_z(\omega) \end{aligned} \tag{10a}$$

$$\begin{aligned} J_y(\omega) = {} & -j\omega\chi_{12}\cos\theta \cdot \varepsilon_0 E_x(\omega) + j\omega(\chi_{11}\cos^2\theta + \chi_{33}\sin^2\theta) \cdot \varepsilon_0 E_y(\omega) \\ & + j\omega(\chi_{33} - \chi_{11})\cos\theta\sin\theta \cdot \varepsilon_0 E_z(\omega) \end{aligned} \tag{10b}$$

$$\begin{aligned} J_z(\omega) = {} & j\omega\chi_{12}\sin\theta \cdot \varepsilon_0 E_x(\omega) + j\omega(\chi_{33} - \chi_{11})\cos\theta\sin\theta \cdot \varepsilon_0 E_y(\omega) \\ & + j\omega(\chi_{11}\sin^2\theta + \chi_{33}\cos^2\theta) \cdot \varepsilon_0 E_z(\omega) \end{aligned} \tag{10c}$$

Substituting constitutive parameters (4) into (10), the coefficients in two sides of (10) can be written as rational fractional functions:

$$\begin{aligned} \sum_{n=0}^{N} g_n(j\omega)^n J_x = {} & \varepsilon_0 \sum_{n=0}^{N} (A_{11\_n}(j\omega)^n E_x + A_{12\_n}(j\omega)^n E_y \\ & + A_{13\_n}(j\omega)^n E_z) \end{aligned} \tag{11a}$$

$$\begin{aligned} \sum_{m=0}^{M} h_m(j\omega)^m J_y = {} & \varepsilon_0 \sum_{m=0}^{M} (A_{21\_m}(j\omega)^m E_x + A_{22\_m}(j\omega)^m E_y \\ & + A_{23\_m}(j\omega)^m E_z) \end{aligned} \tag{11b}$$

$$\begin{aligned} \sum_{m=0}^{M} h_m(j\omega)^m J_z = {} & \varepsilon_0 \sum_{m=0}^{M} (A_{31\_m}(j\omega)^m E_x + A_{32\_m}(j\omega)^m E_y \\ & + A_{33\_m}(j\omega)^m E_z) \end{aligned} \tag{11c}$$

where $N = 2$ and $M = 3$; g_n, h_m, A_{1j_n}, A_{2j_m} and A_{3j_m} ($j = 1, 2, 3$; $n = 0, 1, \ldots N$; $m = 0, 1, \ldots M$.) are as follow

$$\begin{cases} g_0 = \nu_{en}^2 + \omega_b^2, \;\; g_1 = 2\nu_{en}, \;\; g_2 = 1; \\ h_0 = \nu_{en}^3 + \nu_{en}\omega_b^2, \;\; h_1 = 3\nu_{en}^2 + \omega_b^2, \;\; h_2 = 3\nu_{en}, \;\; h_3 = 1; \\ A_{11\_0} = \nu_{en}\omega_p^2, \;\; A_{11\_1} = \omega_p^2, \;\; A_{11\_2} = 0; \\ A_{12\_0} = -\omega_b\omega_p^2 \cos\theta, \;\; A_{12\_1} = 0, \;\; A_{12\_2} = 0; \\ A_{13\_0} = \omega_b\omega_p^2 \sin\theta, \;\; A_{13\_1} = 0, \;\; A_{13\_2} = 0; \\ A_{21\_0} = \nu_{en}\omega_b\omega_p^2 \cos\theta, \;\; A_{21\_1} = \omega_b\omega_p^2 \cos\theta, \;\; A_{21\_2} = A_{21\_3} = 0; \\ A_{22\_0} = \nu_{en}^2\omega_p^2 + \omega_b^2\omega_p^2 \sin^2\theta, \;\; A_{22\_1} = 2\omega_p^2\nu_{en}, \;\; A_{22\_2} = \omega_p^2, \;\; A_{22\_3} = 0; \\ A_{23\_0} = \omega_b^2\omega_p^2 \cos\theta \sin\theta, \;\; A_{23\_1} = A_{23\_2} = A_{23\_3} = 0; \\ A_{31\_0} = -\nu_{en}\omega_b\omega_p^2 \sin\theta, \;\; A_{31\_1} = -\omega_b\omega_p^2 \sin\theta, \;\; A_{31\_2} = A_{31\_3} = 0; \\ A_{32\_0} = \omega_b^2\omega_p^2 \sin\theta \cos\theta, \;\; A_{32\_1} = A_{32\_2} = A_{32\_3} = 0; \\ A_{33\_0} = \nu_{en}^2\omega_p^2 + \omega_b^2\omega_p^2 \cos^2\theta, \;\; A_{33\_1} = 2\omega_p^2\nu_{en}, \;\; A_{33\_2} = \omega_p^2, \;\; A_{33\_3} = 0; \end{cases} \quad (12)$$

It is well known that the transition relation between shift operator z_t and differential operator $\partial/\partial t$ is [13–15]

$$\partial/\partial t \to \left(\frac{2}{\Delta t} \cdot \frac{z_t - 1}{z_t + 1}\right) \quad (13)$$

Transforming Equation (11) to time domain and substituting (13) into the formulae by using the SO-FDTD method, the recursive formulae between **J** and **E** are arranged as

$$J_x^{n+\frac{1}{2}} = \frac{2\varepsilon_0}{p_0}\left(\sum_{i=0}^{2} B_{11\_i}E_x^{n-i} + \sum_{i=0}^{2} B_{12\_i}E_y^{n-i} + \sum_{i=0}^{2} B_{13\_i}E_z^{n-i}\right) - \frac{1}{p_0}\left[(p_0 + p_1)J_x^{n-\frac{1}{2}} + (p_1 + p_2)J_x^{n-\frac{3}{2}} + p_2 J_x^{n-\frac{5}{2}}\right] \quad (14a)$$

$$J_y^{n+\frac{1}{2}} = \frac{2\varepsilon_0}{q_0}\left(\sum_{i=0}^{3} B_{21\_i}E_x^{n-i} + \sum_{i=0}^{3} B_{22\_i}E_y^{n-i} + \sum_{i=0}^{3} B_{23\_i}E_z^{n-i}\right) - \frac{1}{q_0}\left[(q_0 + q_1)J_y^{n-\frac{1}{2}} + (q_1 + q_2)J_y^{n-\frac{3}{2}} + (q_2 + q_3)J_y^{n-\frac{5}{2}} + q_3 J_y^{n-\frac{7}{2}}\right] \quad (14b)$$

$$J_z^{n+\frac{1}{2}} = \frac{2\varepsilon_0}{q_0}\left(\sum_{i=0}^{3} B_{31\_i}E_x^{n-i} + \sum_{i=0}^{3} B_{32\_i}E_y^{n-i} + \sum_{i=0}^{3} B_{33\_i}E_z^{n-i}\right) - \frac{1}{q_0}\left[(q_0 + q_1)J_z^{n-\frac{1}{2}} + (q_1 + q_2)J_z^{n-\frac{3}{2}} + (q_2 + q_3)J_z^{n-\frac{5}{2}} + q_3 J_z^{n-\frac{7}{2}}\right] \quad (14c)$$

In order that the coefficients in above formulae can be presented in simpler forms, we definite two matrices, which are expressed as

$$\hat{\mathbf{N}} = \begin{bmatrix} 1 & \delta & \delta^2 \\ 2 & 0 & -2\delta^2 \\ 1 & -\delta & \delta^2 \end{bmatrix} \tag{15}$$

$$\hat{\mathbf{M}} = \begin{bmatrix} 1 & \delta & \delta^2 & \delta^3 \\ 3 & \delta & -\delta^2 & -3\delta^3 \\ 3 & -\delta & -\delta^2 & 3\delta^3 \\ 1 & -\delta & \delta^2 & -\delta^3 \end{bmatrix} \tag{16}$$

where $\delta = 2/\Delta t$. Then the B_{1i_j}, B_{2i_k}, B_{3i_k}, p_j and q_k ($i = 1, 2, 3$; $j = 0, 1, 2$; $k = 0, 1, 2, 3.$) in (14) can be obtained in the following way:

$$\begin{cases} \begin{bmatrix} p_0 \\ p_1 \\ p_2 \end{bmatrix} = \hat{\mathbf{N}} \cdot \begin{bmatrix} g_0 \\ g_1 \\ g_2 \end{bmatrix}, \quad \begin{bmatrix} B_{1i\_0} \\ B_{1i\_1} \\ B_{1i\_2} \end{bmatrix} = \hat{\mathbf{N}} \cdot \begin{bmatrix} A_{1i\_0} \\ A_{1i\_1} \\ A_{1i\_2} \end{bmatrix} \\ \begin{bmatrix} q_0 \\ q_1 \\ q_2 \\ q_3 \end{bmatrix} = \hat{\mathbf{M}} \cdot \begin{bmatrix} h_0 \\ h_1 \\ h_2 \\ h_3 \end{bmatrix}, \quad \begin{bmatrix} B_{2i\_0} \\ B_{2i\_1} \\ B_{2i\_2} \\ B_{2i\_3} \end{bmatrix} = \hat{\mathbf{M}} \cdot \begin{bmatrix} A_{2i\_0} \\ A_{2i\_1} \\ A_{2i\_2} \\ A_{2i\_3} \end{bmatrix}, \begin{bmatrix} B_{3i\_0} \\ B_{3i\_1} \\ B_{3i\_2} \\ B_{3i\_3} \end{bmatrix} = \hat{\mathbf{M}} \cdot \begin{bmatrix} A_{3i\_0} \\ A_{3i\_1} \\ A_{3i\_2} \\ A_{3i\_3} \end{bmatrix} \end{cases} \tag{17}$$

A direct implementation of (14) would require additional seventeen back storage arrays: E_x^{n-i}, E_y^{n-i}, E_z^{n-i}, $J_y^{n-1/2-i}$, $J_z^{n-1/2-i}$, $J_x^{n-1/2-j}$ ($i = 1, 2, 3$; $j = 1, 2.$), which costs a lot of memory resource. Subsequently, we employ a memory-minimized algorithm [23] to reduce memory requirement. It is seen from (11) that the order of $j\omega$ in the rational polynomial function is lower in comparison with the SO-FDTD method introduced in [22] (for example, the order $N = 4$ and $M = 6$ in [22], $N = 2$ and $M = 3$ in this paper), which is advantageous for reducing the memory storage when adopting the memory-minimized algorithm. Introducing two auxiliary variables J_{x1} and J_{x2}, (14a) can be rewritten in the form of the following three equations:

$$J_x^{n+\frac{1}{2}} = \frac{2\varepsilon_0}{p_0}(B_{11\_0}E_x^n + B_{12\_0}E_y^n + B_{13\_0}E_z^n) - \frac{p_0+p_1}{p_0} temp\_J_x + J_{x1}^{n-\frac{1}{2}} \tag{18a}$$

$$J_{x1}^{n+\frac{1}{2}} = \frac{2\varepsilon_0}{p_0}(B_{11\_1}E_x^n + B_{12\_1}E_y^n + B_{13\_1}E_z^n) - \frac{p_1+p_2}{p_0} temp\_J_x + J_{x2}^{n-\frac{1}{2}} \tag{18b}$$

$$J_{x2}^{n+\frac{1}{2}} = \frac{2\varepsilon_0}{p_0}(B_{11\_2}E_x^n + B_{12\_2}E_y^n + B_{13\_2}E_z^n) - \frac{p_2}{p_0} temp\_J_x \tag{18c}$$

where $temp\_J_x = J_x^{n-1/2}$, which is a temporary storage variable (not a storage array) used to store $J_x^{n-1/2}$. The $J_x^{n-1/2}$ should be calculated and stored in $temp\_J_x$ before the calculation of $J_x^{n+1/2}$

and the implementation order from (18a) to (18c) should be kept unchangeably in the FDTD iterative cycle. Consequently, only two auxiliary storage variables (J_{x1} and J_{x2}) per cell in the problem space are required to obtain J_x from **E**, which saves eight back storage arrays more than the direct implementation of (14a). Similarly, by denoting $temp\_J_y = J_y^{n-1/2}$ and introducing three auxiliary variables J_{y1}, J_{y2} and J_{y3}, (14b) can be rewritten as

$$J_y^{n+\frac{1}{2}} = \frac{2\varepsilon_0}{q_0}(B_{21\_0}E_x^n + B_{22\_0}E_y^n + B_{23\_0}E_z^n) - \frac{q_0+q_1}{q_0}temp\_J_y + J_{y1}^{n-\frac{1}{2}} \quad (19a)$$

$$J_{y1}^{n+\frac{1}{2}} = \frac{2\varepsilon_0}{q_0}(B_{21\_1}E_x^n + B_{22\_1}E_y^n + B_{23\_1}E_z^n) - \frac{q_1+q_2}{q_0}temp\_J_y + J_{y2}^{n-\frac{1}{2}} \quad (19b)$$

$$J_{y2}^{n+\frac{1}{2}} = \frac{2\varepsilon_0}{q_0}(B_{21\_2}E_x^n + B_{22\_2}E_y^n + B_{23\_2}E_z^n) - \frac{q_2+q_3}{q_0}temp\_J_y + J_{y3}^{n-\frac{1}{2}} \quad (19c)$$

$$J_{y3}^{n+\frac{1}{2}} = \frac{2\varepsilon_0}{q_0}(B_{21\_3}E_x^n + B_{22\_3}E_y^n + B_{23\_3}E_z^n) - \frac{q_3}{q_0}temp\_J_y \quad (19d)$$

It is seen from (19) that significant savings in the memory storage is achieved with respective to the direct computation of (14b). Similar method can be used for solving (14c), which is shown as follows:

$$J_z^{n+\frac{1}{2}} = \frac{2\varepsilon_0}{q_0}(B_{31\_0}E_x^n + B_{32\_0}E_y^n + B_{33\_0}E_z^n) - \frac{q_0+q_1}{q_0}temp\_J_z + J_{z1}^{n-\frac{1}{2}} \quad (20a)$$

$$J_{z1}^{n+\frac{1}{2}} = \frac{2\varepsilon_0}{q_0}(B_{31\_1}E_x^n + B_{32\_1}E_y^n + B_{33\_1}E_z^n) - \frac{q_1+q_2}{q_0}temp\_J_z + J_{z2}^{n-\frac{1}{2}} \quad (20b)$$

$$J_{z2}^{n+\frac{1}{2}} = \frac{2\varepsilon_0}{q_0}(B_{31\_2}E_x^n + B_{32\_2}E_y^n + B_{33\_2}E_z^n) - \frac{q_2+q_3}{q_0}temp\_J_z + J_{z3}^{n-\frac{1}{2}} \quad (20c)$$

$$J_{z3}^{n+\frac{1}{2}} = \frac{2\varepsilon_0}{q_0}(B_{31\_3}E_x^n + B_{32\_3}E_y^n + B_{33\_3}E_z^n) - \frac{q_3}{q_0}temp\_J_z \quad (20d)$$

where $temp\_J_z = J_z^{n-1/2}$, and J_{z1}, J_{z2} and J_{z3} are three auxiliary storage arrays needed to store field components for the problem space.

From formulae mentioned above, there comes a conclusion of the computation processes by the SO-FDTD:

(a) From formula (7), **H** is derived from **E**;
(b) From formulae (18), (19) and (20), **J** is derived from **E**;
(c) From formula (8), **E** is derived from **H**;
(d) According to the sequences of (a), (b) and (c), a recursion is completed and next recursion begins.

In addition, all coefficients are computed prior to the FDTD iterative cycle of the field computation to save computational time.

To illuminate the validity of the proposed new SO-FDTD method in saving memory requirement, we compared the number of storage arrays used to store field quantities between three SO-FDTD methods, i.e., the proposed SO-FDTD method in this paper, the original SO-FDTD method (here, referring to that the implementation scheme is the same as that of the new SO-FDTD method provided in this paper but without a combination of the memory-minimized algorithm) and the SO-FDTD method in kDB coordinates system introduced in [22]. In order to construct the same case as that in kDB coordinates system, we suppose the direction of incident EM-wave parallel to the

Table 1. Comparison of the number of storage arrays used for different SO-FDTD methods in the 1D/3D problem space.

FDTD method		New SO-FDTD method in this paper (using the memory-minimized algorithm)							
3D	Field components	J_x	J_y	J_z	E_x	E_y	E_z	H_x	H_y
	The number of storage arrays used for each field	3	4	4	1	1	1	1	1
	Total number of the storage arrays	16							
FDTD method		Original SO-FDTD method in this paper (without using the memory-minimized algorithm)							
3D	Field components	J_x	J_y	J_z	E_x	E_y	E_z	H_x	H_y
	The number of storage arrays used for each field	4	5	5	5	5	5	1	1
	Total number of the storage arrays	31							
FDTD method		SO-FDTD method proposed in [22] (based on the kDB coordinates system)							
3D	Field components	D_1	D_2	E_1	E_2	E_3	H_1	H_2	
	The number of storage arrays used for each field	7	7	5	7	7	1	1	
	Total number of the storage arrays	35							

FDTD method		New SO-FDTD method in this paper (using the memory-minimized algorithm)							
1D	Field components	J_x	J_y	J_z	E_x	E_y	E_z	H_x	H_y
	The number of storage arrays used for each field	3	4	4	1	1	1	1	1
	Total number of the storage arrays	16							
FDTD method		Original SO-FDTD method in this paper (without using the memory-minimized algorithm)							
1D	Field components	J_x	J_y	J_z	E_x	E_y	E_z	H_x	H_y
	The number of storage arrays used for each field	4	5	5	5	5	5	1	1
	Total number of the storage arrays	31							
FDTD method		SO-FDTD method proposed in [22] (based on the kDB coordinates system)							
1D	Field components	D_1	D_2	E_1	E_2	E_3	H_1	H_2	
	The number of storage arrays used for each field	7	7	5	7	0	1	1	
	Total number of the storage arrays	28							

z axis and the steady biasing magnetic field at an angle θ with respect to the z axis, thus there is no need to calculate H_z component for the SO-FDTD method based on Cartesian coordinates system. The number of storage arrays used for above mentioned three SO-FDTD methods to calculate the magnetized plasma with arbitrary magnetic declination in the three-dimensional (3D) and one-dimensional (1D) problem space are analyzed and summarized in Table 1. It is apparent from the Table 1 that, for the novel SO-FDTD method proposed in this work, the number of storage variables per cell in either 3D or 1D FDTD problem region is greatly reduced as compared to the original SO-FDTD method and the SO-FDTD method based on the kDB coordinates system provided in [22]. As for 2D problem space, there is also the greatest enhancement in saving memory storage for our

proposed improved SO-FDTD method, which can be easily obtained through some deduction.

3. NUMERICAL VERIFICATION

To demonstrate the validity of the aforementioned recently improved SO-FDTD method, we compute the reflection and transmission coefficients of electromagnetic wave through a uniform magnetized collision plasma slab. This simple example is chosen because exact analytical solutions are available. As shown in Figure 1, the incident wave normally impinges on a magnetized plasma slab with arbitrary magnetic declination. The computational domain is subdivided into 450 cells, and the plasma occupies cells 200–320. Each cell is 75 μm long, so the plasma layer is 9.0 mm thick. Five-cell PML (Perfectly Matched Layer) medium is applied at the terminations of the space to eliminate unwanted reflections, and the remainder is free space. To satisfy courant stability condition, the time step Δt is set as 0.125 ps. The incident wave used in the simulation is a Gaussian-derivative pulsed plane wave: $E_{inc} = (t - t_0)/\tau \times \exp[-4 \times \pi(t - t_0)^2/\tau^2]$, where $t_0 = 70\Delta t$, $\tau = 140\Delta t$. Parameters of the plasma are: $\omega_p = 50 \times 2\pi \times 10^9$ rad/s, $\omega_b = 3 \times 10^{11}$ rad/s, $\nu_{en} = 2 \times 10^{10}$ Hz. To validate the accuracy of the SO-FDTD method, comparisons with the analytical results and other numerical methods are needed.

The electric fields data are recorded at cell 199 and cell 321 and then transformed to the frequency domain through discrete Fourier transform (DFT). From the FDTD data, the reflection and transmission coefficients are achieved by:

$$R(\omega) = [E_{xr}(\omega) + \xi \cdot E_{yr}(\omega)]/E_{xi}(\omega) \quad (21)$$

$$T(\omega) = [E_{xt}(\omega) + \xi \cdot E_{yt}(\omega)]/E_{xi}(\omega) \quad (22)$$

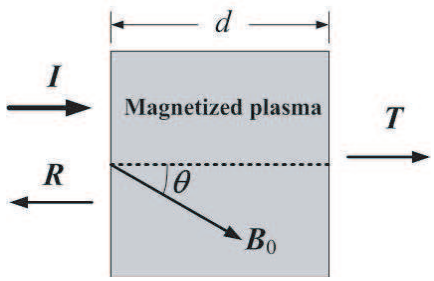

Figure 1. The EM-problem model of a plane wave normally incident on a magnetized plasma slab.

where

$$E_{xr}(\omega) = DFT[E_{xt}(t) - E_{xi}(t)], \quad E_{yr}(\omega) = DFT[E_{yt}(t) - E_{yi}(t)]$$
$$E_{xt}(\omega) = DFT[E_{xt}(t)], \quad E_{yt}(\omega) = DFT[E_{yt}(t)]$$

The subscripts i, r, t correspond to the incident field, the reflected one and the total one, respectively. For a magnetized plasma with an arbitrary angle θ between wave vector $\mathbf{k}$ and bias magnetic field $\mathbf{B}_0$, ξ in above equations satisfies such a relation as follows [24]:

$$\xi = -\frac{j}{\cos\theta} \cdot \left[\frac{\frac{\omega_b}{\omega}\sin^2\theta}{2\left(1 - j\frac{\nu_{en}}{\omega} - \frac{\omega_p^2}{\omega^2}\right)} \pm \sqrt{\frac{\frac{\omega_b^2}{\omega^2}\sin^4\theta}{4\left(1 - j\frac{\nu_{en}}{\omega} - \frac{\omega_p^2}{\omega^2}\right)^2} + \cos^2\theta} \right] \quad (23)$$

For the specific case $\theta = 0°$, $\xi = \pm j$, where "$-$" sign is for left-hand circularly polarization (LCP) wave while "$+$" sign represents right-hand circularly polarization (RCP) wave.

The reflection and transmission coefficients versus frequency obtained by the improved SO-FDTD method, the SO-FDTD method introduced in [22] (For simplicity, we called this method as the kDB-SO-FDTD method) and the analytical method for $\theta = 0°$ are shown in Figures 2 and 3. As far as the analytical solutions are concerned, we follow the method found in Ginzburg [24]. It is known that the Eigen wave in this case becomes two types of circularly polarized waves: LCP wave and RCP wave. From these figures, it is found that the agreements between the improved SO-FDTD method, the kDB-SO-FDTD method and the analytical values are quite well. Furthermore,

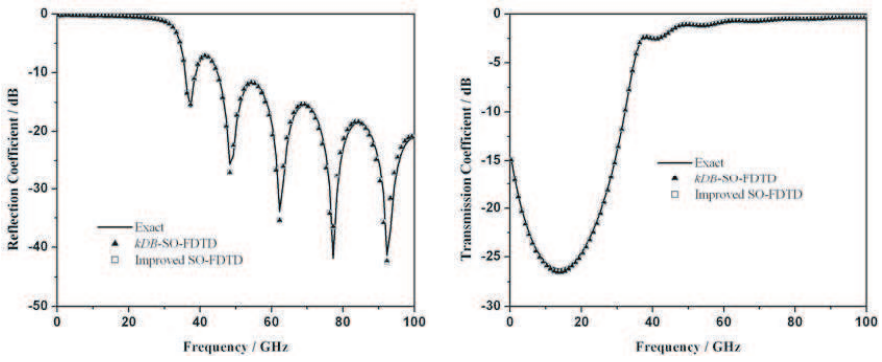

Figure 2. LCP wave reflection and transmission coefficient magnitude vs. frequency of the anisotropic magnetized plasma. (a) Reflection coefficient. (b) Transmission coefficient.

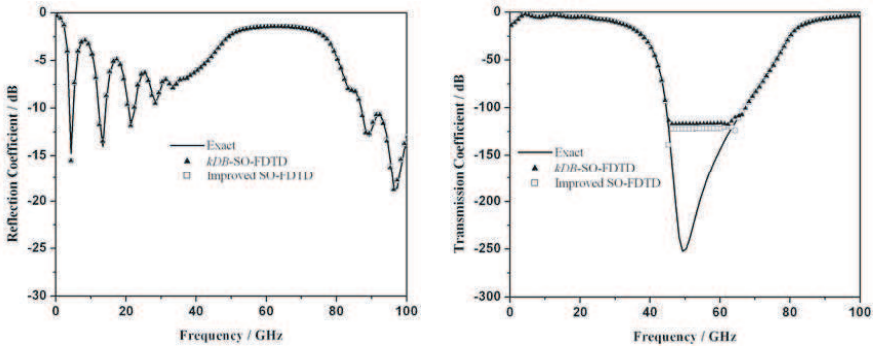

(a) (b)

Figure 3. RCP wave reflection and transmission coefficient magnitude vs. frequency of the anisotropic magnetized plasma. (a) Reflection coefficient. (b) Transmission coefficient.

the accuracy of the improved SO-FDTD method is a little better than that of the kDB-SO-FDTD method, which can be seen from the transmission coefficient for RCP wave shown in Figure 3(b). However, one can find that there is a distinct deviation between numerical and analytical results in Figure 3(b). The reason is that there exists a stop-band in the frequency spectrum where the wavenumber is pure imaginary and no waves at these frequencies can propagate [5]. It also can be seen that the characteristics of RCP wave and LCP wave propagating through magnetized plasma are significantly different, which has be discussed in detail in [22], and we do not discuss a lot about it here.

When EM-wave propagates through uniform magnetized plasma plate with a magnetic declination angle θ between 0° and 90°, there are two kinds of eigen waves in this case, which are both elliptically polarized waves. One is called first type wave (I-wave) where the "+" sign is taken in Equation (23), and the other is second type wave (II-wave) where the "−" sign is taken in Equation (23). Suppose θ is set to 45° and 65°, the reflection coefficient and transmission coefficient vs. frequency for I-wave and II-wave computed using the improved SO-FDTD and kDB-SO-FDTD methods are compared to the exact solutions in Figures 4 and 5. It is shown from the numerical results that the improved SO-FDTD method coincides with the analytical method very well and is more accurate than the kDB-SO-FDTD method, which can be seen in Figure 5(b) where the improved SO-FDTD method solution follows the analytical curve more deeply during the stop-band in comparison with the kDB-SO-FDTD

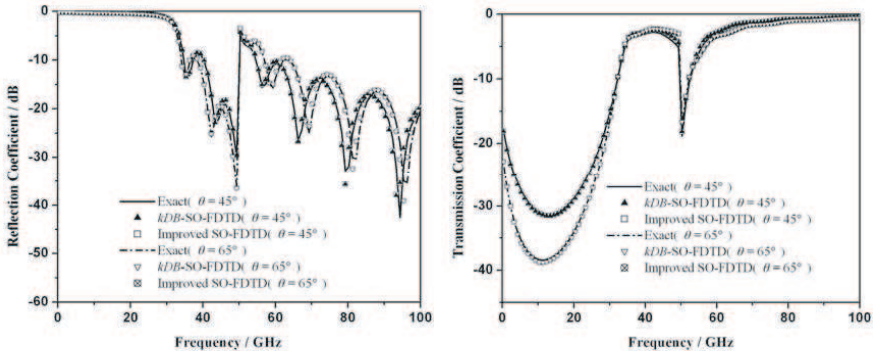

(a) (b)

Figure 4. I-wave reflection and transmission coefficient magnitude in anisotropic plasma for $\theta = 45°$ and $\theta = 65°$ respectively. (a) Reflection coefficient. (b) Transmission coefficient.

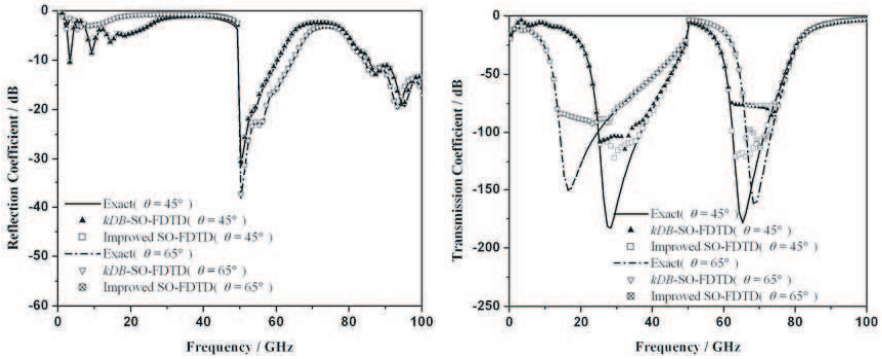

(a) (b)

Figure 5. II-wave reflection and transmission coefficient magnitude in anisotropic plasma for $\theta = 45°$ and $\theta = 65°$ respectively. (a) Reflection coefficient. (b) Transmission coefficient.

method. However, the improved SO-FDTD method also has trouble in predicting transmission coefficient values for II-wave where the stop-band exists in the frequency spectrum.

It can be noticed from Figures 4 and 5 that I-wave is left-handed elliptically polarized wave and possesses the property similar to LCP wave and II-wave is right-handed elliptically polarized wave whose feature is alike that of RCP wave. There is a sudden change at the point of plasma frequency for both I-wave and II-wave, which can be explained by the fact that the plasma frequency is inherently one of

reflection points.

Regarding computation efficiency, we have conducted a test on the EM-problem model where the EM-wave propagates through a uniform magnetized plasma slab with a magnetic declination angle of 45°. The simulation parameters are the same as the above EM-problem model of $\theta = 45°$, but the computational domain is changed with three cases. In Case 1, the FDTD problem space consists of 450 cells with the magnetized plasma occupying cells 200–320. In Case 2, the computational space is subdivided into 1000 cells and the plasma occupies cells from 200 to 800. In Case 3, the computational space consists of 1600 cells with the plasma situated on cells 200–1400. The simulations were allowed to run for 10000 time steps by a computer based on Intel(R) Core(TM) i5-2400 CPU @ 3.10 GHz. The time cost of computing by the improved SO-FDTD method and the kDB-SO-FDTD method is shown in Table 2. It should be noticed that the programs of the two FDTD methods had been carried out for six times to gain the average time cost for each case. The data shown in Table 2 indicate that the machine time of the improved SO-FDTD method is much less than that of the kDB-SO-FDTD method. The more space cells occupied by the magnetized plasma, the more reduction in running time is achieved by the improved SO-FDTD method. From the derivation of the existing FDTD methods, it is easy to find the reasons why the new SO-FDTD method is more efficient and accurate than the kDB-SO-FDTD method. The first reason is that the storage arrays used for the proposed scheme are less than that of the kDB-SO-FDTD method due to the lower order of $j\omega$ in the rational polynomial function and the incorporation of the memory-minimized algorithm. As a result, the accumulated error is decreased and the computation time is saved. The second possible reason is that the recursion formulae of the improved SO-FDTD method are deduced and programmed easily. For instance, compared to the kDB-SO-FDTD method, the recursive formulae between $\mathbf{J}$ and $\mathbf{E}$ introduced in this paper is simpler than that between $\mathbf{D}$ and $\mathbf{E}$.

Table 2. Comparison of the average running times used for the new SO-FDTD method and the kDB-SO-FDTD method proposed in [22]. (Each program was allowed to run for six times to obtain an average time cost).

	Case 1	Case 2	Case 3
the new SO-FDTD method	1.7120 s	3.5448 s	5.7983 s
the kDB-SO-FDTD method	1.7411 s	4.0371 s	6.8468 s

4. CONCLUSION

In this paper, a new SO-FDTD method for modeling the anisotropic dispersive magnetized plasma with arbitrary magnetic declination is derived using the discrete difference schemes about **J**, **E** and **H** and a memory-minimized technique. Then, this method is applied to calculating the reflection and transmission coefficients of electromagnetic wave through a magnetized plasma layer and its accuracy is validated by the analytical method. Compared to the SO-FDTD method in kDB coordinates system proposed in [22], our proposed method is more accurate and efficient. As for formulae derivation, the recursion formulae of the improved SO-FDTD method are deduced and programmed easily and they involve no complex variables, so the computations become simpler in comparison with other FDTD algorithm based on recursive convolution or transformation principle such as the methods in [19–21]. Therefore, the improved SO-FDTD method proposed in this paper is advantageous for decreasing accumulated error and saving computation time in calculating anisotropic magnetized plasma with arbitrary magnetic declination. Though only one-dimensional examples are discussed in this paper, this novel SO-FDTD method can be easily extended to resolve two- or three-dimensional problems for anisotropic magnetized plasma and can be used in other frequency dispersion electromagnetic problem if it is modified slightly.

ACKNOWLEDGMENT

The authors are obliged to the National Natural Science Foundation of China for Grant 40974092.

REFERENCES

1. Pu, T.-L., K.-M. Huang, B. Wang, and Y. Yang, "Application of micro-genetic algorithm to the design of matched high gain patch antenna with zero-refractive-index metamaterial lens," *Journal of Electromagnetic Waves and Applications*, Vol. 24, No. 8–9, 1207–1217, 2010.
2. Young, J. L., "A full finite difference time-domain implementation for radio wave propagation in plasma," *Radio Sci.*, Vol. 29, 1513–1522, 1994.
3. Kelley, D. F. and R. J. Luebbers. "Piecewise linear recursive convolution for dispersive media using FDTD," *IEEE Trans. Antennas Propag.*, Vol. 44, No. 6, 792–797, 1996.

4. Ai, X., Y. Han, C. Y. Li, and X.-W. Shi, "Analysis of dispersion relation of piecewise linear recursive convolution FDTD method for space-varying plasma," *Progress In Electromagnetics Research Letters*, Vol. 22, 83–93, 2011.
5. Huang, S. and F. Li, "Time domain analysis of transient propagation in inhomogeneous magnetized plasma using Z-transforms," *Journal of Electronics (China)*, Vol. 23, No. 1, 113–116, 2006.
6. Shibayama, J., R. Takahashi, A. Nomura, J. Yamauchi, and H. Nakano, "Concise frequency-dependent formulation for LOD-FDTD method using Z transforms," *Electronics Letters*, Vol. 44, No. 16, 949–950, 2008.
7. Liu, S., M. Liu, and W. Hong, "Modified piecewise linear current density recursive convolution finite-difference time-domain method for anisotropic magnetized plasma," *IET Microw. Antennas Propag.*, Vol. 2, No. 7, 677–685, 2008.
8. Shibayama, J., R. Ando, A. Nomura, J. Yamauchi, and H. Nakano, "Simple trapezoidal recursive convolution technique for the frequency-dependent FDTD analysis of a Drude-Lorentz model," *IEEE Photonics Technology Letters*, Vol. 21, 100–102, 2009.
9. Liu, S., S. Liu, and S. Liu, "Analysis for scattering of conductive objects covered with anisotropic magnetized plasma by trapezoidal recursive convolution finite-difference time-domain method," *Int. J. RF and Microwave CAE*, Vol. 20, 465–472, 2010.
10. Ramadan, O, "Unsplit field implicit PML algorithm for complex envelope dispersive LOD- FDTD simulations," *Electronics Letters*, Vol. 43, No. 5, 17–18, 2007.
11. Tan, E. L., "Acceleration of LOD-FDTD method using fundamental scheme on graphics processor units," *IEEE Microwave Theory and Techniques Society*, Vol. 20, No. 12, 648–650, 2010.
12. Yang, L., Y. Xie, and P. Yu, "Study of bandgap characteristics of 2D magnetoplasma photonic crystal by using M-FDTD method," *Microwave and Optical Technology Letters*, Vol. 53, No. 8, 1778–1784, 2011.
13. Attiya, A. M. and H. H. Abdullah, "Shift-operator finite difference time domain: An efficient unified approach for simulating wave propagation in different dispersive media," *IEEE Middle East Conference on Antennas and Propagation*, 1–4, 2010.
14. Wang, F., B. Wei, and D.-B. Ge, "A method for FDTD modeling of wave propagation in magnetized plasma," *International Conference on Consumer Electronics, Communications and Networks*, 4659–4662, 2011.

15. Ma, L.-X., H. Zhang, et al., "Improved finite difference time-domain method for anisotropic magnetised plasma based on shift operator," *IET Microw. Antennas Propag.*, Vol. 4, No. 9, 1442–1447, 2010.
16. Cereceda, C., M. De Peretti, and C. Deutsch, "Stopping power for arbitrary angle between test particle velocity and magnetic field," *Phys. Plasmas*, Vol. 12, 022102, 2005.
17. Nersisyan, H. B., C. Toepffer, and G. Zwicknagel, *Interaction between Charged Particles in a Magnetic Field: A Theoretical Approach to Ion Stopping in Magnetized Plasmas,* Springer-Verlag, Heidelberg and New York, 2007.
18. Deutsch, C. and R. Popoff, "Low velocity ion slowing down in a strongly magnetized plasma target," *Phys. Rev.*, Vol. E78, 056405, 2008.
19. Xu, L. J., and N. C. Yuan, "FDTD formulations for scattering from 3-D anisotropic magnetized plasma objects," *IEEE Ant. & Wireless Propagt. Letters*, Vol. 5, 335–338, 2006.
20. Qian, Z. H. and R. S. Chen, "FDTD analysis of magnetized plasma with arbitrary magnetic declination," *International Journal of Infrared and Millimeter Waves*, Vol. 28, No. 5, 815–825, 2007.
21. Yang, L.-X., Y.-J. Wang, and G. Wang, "A 3D FDTD implementation of electromagnetic scattering by magnetized plasma medium based on laplace transfer principle," *Acta Electronica Sinica (China)*, Vol. 37, No. 12, 2711–2715, 2009.
22. Ma, L.-X., H. Zhang, et al., "Shift-operator FDTD method for anisotropic plasma in kDB coordinates system," *Progress In Electromagnetics Research M*, Vol. 12, 51–65, 2010.
23. Li, J. and J. Dai, "An efficient implementation of the stretched coordinate perfectly matched layer," *IEEE Microwave and Wireless Components Letters*, Vol. 17, No. 5, 322–324, 2007.
24. Ginzburg, V. L., *The Propagation of Electromagnetic Waves in Plasmas,* 2nd edition, Ch. 6, Pergamon, New York, 1970.